

Supplementary Material

Free energy recovery in single molecule experiments

Single molecule force measurements (experimental setup shown in Fig. S1) can be used to determine free-energy differences between the folded (F) and the unfolded (U) states provided that the process is quasi-static (i.e. that the pulling is done slowly enough for the system to go through a succession of equilibrium states). In the mechanical unfolding of an RNA molecule, by measuring the reversible work W_{rev} performed on the molecule during the unfolding process and using the thermodynamic relation $\Delta G = W_{rev}$, we can estimate the RNA folding free energy at zero force ΔG_0 (after correcting for the stretching of the handles required to manipulate the RNA hairpin and the entropy loss of the RNA between the extended conformation at a fixed end-to-end distance and the unfolded state). This method has been applied to small RNA hairpins that, in the absence of Mg^{++} , can be unfolded quasi-statically at low pulling speeds¹. However, when the native state is determined by the existence of tertiary contacts, pulling cannot be carried out reversibly as the typical value of the folding-unfolding relaxation time τ_{relax} (measured at the transition force, $F_{1/2}$, i.e. the force at which both chemical species (F,U) are equally populated) is larger than the time required to reach $F_{1/2}$ during the pulling protocol, $\tau_{relax} \gg F_{1/2} / r$, where r is the loading rate in pN-s⁻¹. Using very low pulling rates is often not a solution to obtain reliable free-energy estimates because of thermal drift of the instrument². Nonequilibrium methods offer an alternative way to extract free energy differences.

The Jarzynski equality

For irreversible pulls it is possible to use the Jarzynski equality³ (hereafter referred to as JE). It relates the equilibrium free-energy difference ΔG between two equilibrium states to an exponential average (denoted by $\langle \dots \rangle$) of the work done on the system, W , taken over an infinite number of repeated nonequilibrium experiments, $\exp(-\Delta G / k_B T) = \langle \exp(-W / k_B T) \rangle$. Using Jensen's inequality, $\log(\langle \exp(X) \rangle) \geq \langle X \rangle$, it follows that $\langle W \rangle \geq \Delta G$ which is recognized as the content of the second law of thermodynamics. For reversible processes the equality holds $\langle W \rangle = \Delta G$. The JE requires exponential averaging over an infinite number of work trajectories in order to recover the free energy. Performing this average over a finite number of trajectories introduces a systematic bias in the free-energy estimate whose magnitude depends on the finite number of pulls and the extent of the work dissipation^{6,7,8}. Recently, the JE was experimentally tested in single-molecule force-unfolding experiments¹ on the P5ab RNA hairpin, a derivative of the L-21 Tetrahymena ribozyme⁴. These experiments showed that application of the Jarzynski equality on work values obtained when the molecule was unfolded irreversibly converged after a few hundred realizations towards the values of the free energy derived from the quasi-static, mechanical unfolding of the molecule. A few hundred repetitions of the irreversible work trajectories were enough to determine the value of ΔG with an accuracy of $\pm \frac{1}{2} k_B T$. This result has been later theoretically justified in⁵. However, the average value of the dissipated work (defined as $W_{diss} = W - \Delta G$) during these irreversible studies was

relatively small, $\sim 3k_B T$, in comparison with values in the range $10 - 50k_B T$ often seen in single molecule pulling experiments, and application of the JE to more dissipative processes is not straightforward. In fact, sources of random noise introduce a systematic bias in the exponential average required by the JE, which can be comparable in magnitude but of different sign to the bias arising from the finite number of pulling repetitions^{6,7,8}. These two sources of noise often lead to large statistical uncertainties in the free energies estimated with the JE, particularly when the process occurs far from equilibrium. We find that the slow convergence shown by the JE can be improved by using the CFT⁹, and that the latter constitutes a less error-sensitive and faster – convergence method to extract equilibrium free energies from non-equilibrium processes. In practice, as mentioned above, it is often difficult to extract unfolding free energies using quasi-static pulling rates (below a few $\text{pN}\cdot\text{s}^{-1}$) due to spatial drift in various components of the manipulation instrument. Drift effects decrease noticeably for larger pulling speeds, making it possible to obtain more reliable experimental data and better statistics (doing a large number of pulls), but at the expense of a more irreversible unfolding process

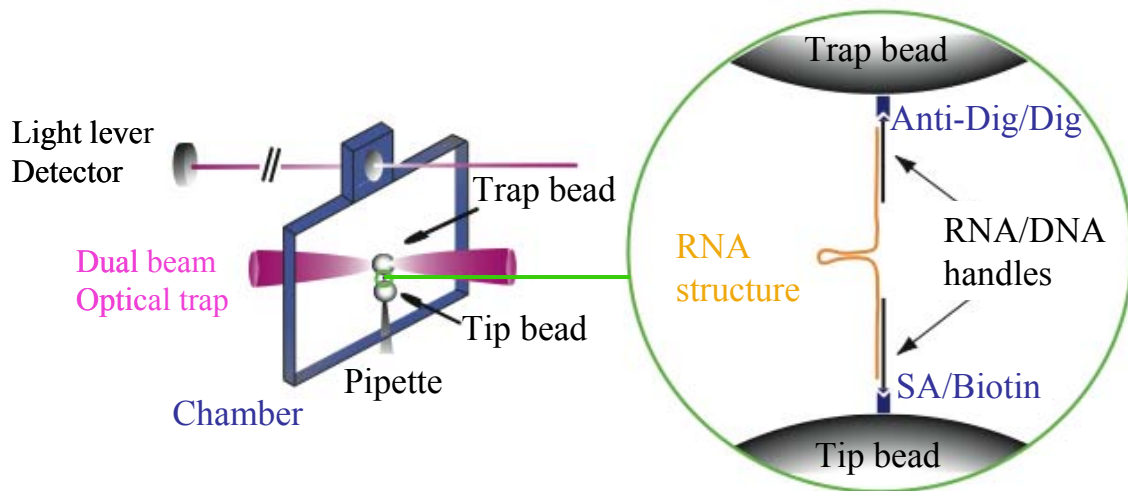


FIGURE S1

Figure S1. The optical tweezers set-up is similar to the one previously described in¹. An RNA molecule is attached between a streptavidin coated bead positioned at the tip of a micropipette and an anti-digoxigenin coated bead captured in an optical trap. A piezo controls the position of the chamber and thus of the bead on the micropipette². Molecules are stretched and relaxed by moving the chamber in the vertical direction at constant rate via the piezoelectric stage. The forces on the trap bead are determined by measuring the change of momentum of the photons as they pass through the trap. This movement is monitored with the light-lever, which consists of a small laser, a lens connected to the chamber, and a detector². Force and extension of the molecule were monitored at ~300 Hz.

The Crooks fluctuation theorem (CFT)

(numbering of equations in this section refer to the body text of the paper)

The reversible process is an example of the CFT (1) where there is no hysteresis, so both unfolding and refolding distributions are equal and $W = \Delta G$. The JE can also be obtained as a particular case of (1) as can be shown by rewriting (1) in the form $P_U(W) \exp(-W / k_B T) = P_R(-W) \exp(-\Delta G / k_B T)$ and integrating with respect to W from $W = -\infty$ to $W = \infty$. The l.h.s of this equation gives then the exponential average of the work along the unfolding path whereas the rhs is equal to $\exp(-\Delta G / k_B T)$.

Expression for the work (2) is not strictly accurate. The CFT (1) requires that x_i must be the control (non-fluctuating) parameter that characterizes the state of the system. However, the end-to-end distance is strictly speaking not the control parameter in our RNA pulling experiments, as the position of the bead fluctuates in the trap^{10,11}. However, it can be shown that this effect is too small compared to other sources of error and the

work done can be approximated¹⁰ by Eq. 2. When this is not the case, the correct free-energy profile can nevertheless be reconstructed using the analysis of Hummer and Szabo¹², or for sufficiently stiff traps the method of Park and Schulten⁷.

Although the simple identity (3) already gives an estimate of ΔG , it is not necessarily very precise as it only uses the local behavior of the distribution around $W = \Delta G$. However, the CFT suggests at least two methods of utilizing the full distributions of work values to extract ΔG and to avoid the noise and the convergence problems of the JE. In the direct method, we plot the ratio $P_U(W)/P_R(-W)$ in logarithmic scale as a function of W . The resulting points should fall on the line $(W - \Delta G)/k_B T$ intersecting the W -axis at $W = \Delta G$; this is a direct test of the validity of the CFT, Eq. (1). When the overlapping region of work values between the unfolding and refolding distributions is too narrow, as may happen for large dissipated work values, the direct method cannot be used and another type of analysis is required. In the matching method we define the functions $g_U(W) = \log(P_U(W)) - W/(2k_B T)$ and $g_R(W) = \log(P_R(-W)) + W/(2k_B T)$ and use Eq. (1) to infer the relation $g_R(W) - g_U(W) = \Delta G/k_B T$. We then determine the value of ΔG such that the experimental distributions $g_U(W), g_R(W)$ match each other. Matching the experimental distributions $g_U(W), g_R(W)$ cannot be very accurate in the presence of large statistical fluctuations in the tails of the distributions. Therefore a different optimization analysis of the experimental data is necessary. This is the basis of the ratio acceptance method developed by Bennett to efficiently estimate free-energy differences from Monte Carlo data^{13,14,15} (see below and Fig. S7). This method has been used to determine values of ΔG that are in agreement (within the statistical error) with the ones

found by the matching method. The values so obtained are comparable (but also more accurate) to those derived by averaging the JE estimates for the unfolding and refolding paths thereby proving the consistency between the different estimates^{13,14}. A compendium of all results obtained for the different molecules we investigated is shown in Table 1 (main text).

Results for the hairpin

For a given pulling speed, systematic deviations in the distributions for different molecules are expected, either due to accumulative drift effects in the optical tweezers machine, or to variability in the tether attachments of the RNA to the beads. These deviations cannot be too large, otherwise the reliability of the method would be compromised. As shown in Fig. S2 variability from molecule to molecule is small allowing us to test Eq. (1) by using data averaged over different molecules. We test the direct method in Fig. S3 where we plot the logarithm of the left hand side of Eq. (1) as a function of $W / k_B T$ for four different molecules, as well as the data averaged over all four molecules. Data for all molecules follow straight lines with slopes in the range 0.8-1.1 and the value of ΔG fluctuates from molecule to molecule within a range of work values which is smaller than $1k_B T$. The average data (green circles) fall on a straight line with a slope 0.95 ± 0.15 —the error being due to variation of the slope among the different molecules—in very good agreement with the expected result. The reported values for $\Delta G^{(\text{exp})} = 110.3 \pm 0.5 k_B T$ are in agreement with estimates obtained using Bennett's acceptance ratio method (Figure S7).

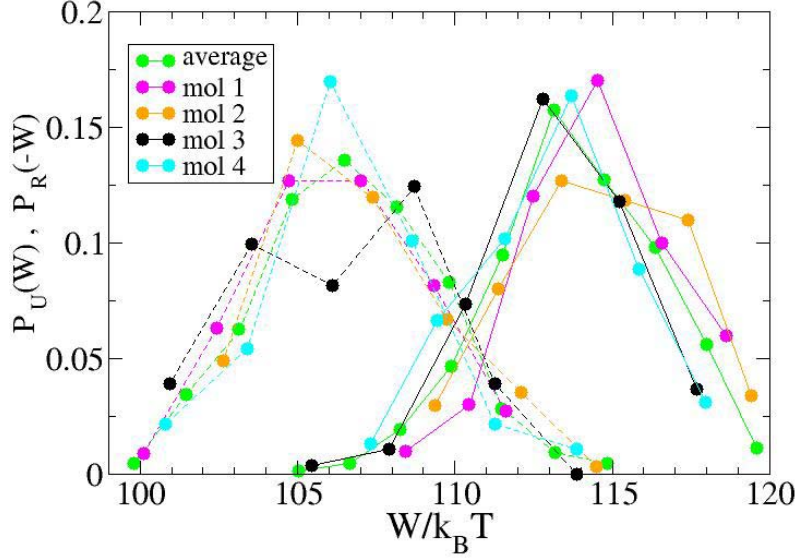


FIGURE S2

Figure S2. Reproducibility of work distributions for 4 molecules taken at $r=7.5\text{pN/s}$. Molecules 1,2,3,4 plotted with different colors correspond to 50,120,110,106 pulls respectively. The thick green line corresponds to the average work distribution (green) shown in Figure 1 (main text).

The result $\Delta G^{(\text{exp})} = 110.3 \pm 0.5 k_B T$ is also in good agreement with estimates obtained using cumulant expansions¹⁶, valid for distributions that do not deviate much from Gaussian behavior. Estimates obtained by using the JE are also comparable, albeit their statistical fluctuations tend to be larger. As shown in the last column of Table 1 (main text), the work distributions for the unfolding of this hairpin satisfy the fluctuation-dissipation relation between the variance of the work and the average dissipated work, $\sigma_{U,R}^2 = 2k_B T W_{dis}^{U,R}$, characteristic of Gaussian work distributions. We note, however, that these irreversible measurements are not taken in the linear response regime. For the latter

we would expect $W_{dis}^{U,R}$ and the variance $\sigma_{U,R}^2$ to be proportional to the loading rate r^5 .

This proportionality is not observed in the data shown in Table 1 (main text), indicating that the dissipated work tends to saturate as has been predicted in two-state kinetic models of the unfolding reaction¹⁷.

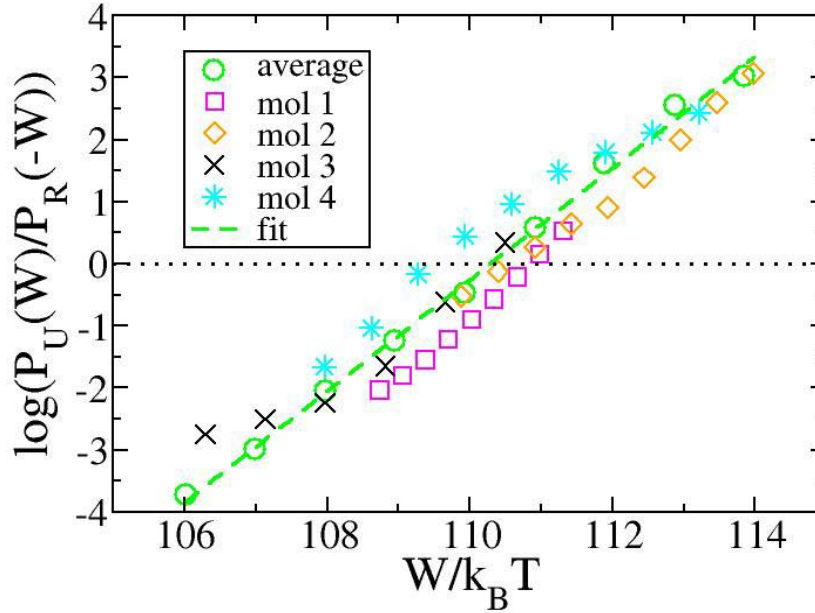


FIGURE S3

Figure S3. Test of the CFT (1) for the distributions shown in Figure S2 plotted in the region of work values W where unfolding and refolding distributions overlap along the work axis (data have been linearly interpolated between contiguous bins of the unfolding and refolding work distributions). The different color symbols correspond to different molecules (same as in Fig. S2), the green color indicating the average data (circles) as well as the best linear fit to that data (dashed green line) giving a slope of 0.95 ± 0.15 (the error spanning the range of slopes observed for different molecules) and a free-energy value $\Delta G^{(\text{exp})} = 110.3 \pm 0.5 k_B T$ (the error being given by the range of work values at which different molecules cross the work axis).

The RNA motif S15

The structure and typical force-extension curves for the wild and mutant types (without magnesium) are shown in Fig.S4 and in Fig. S5 for the wild type in magnesium. The matching method shown in Fig. S6 makes it possible to determine the value of ΔG for the unfolding of both molecules without magnesium. Folding free energy predictions for S15 under different conditions are given in Table 1 (main text).

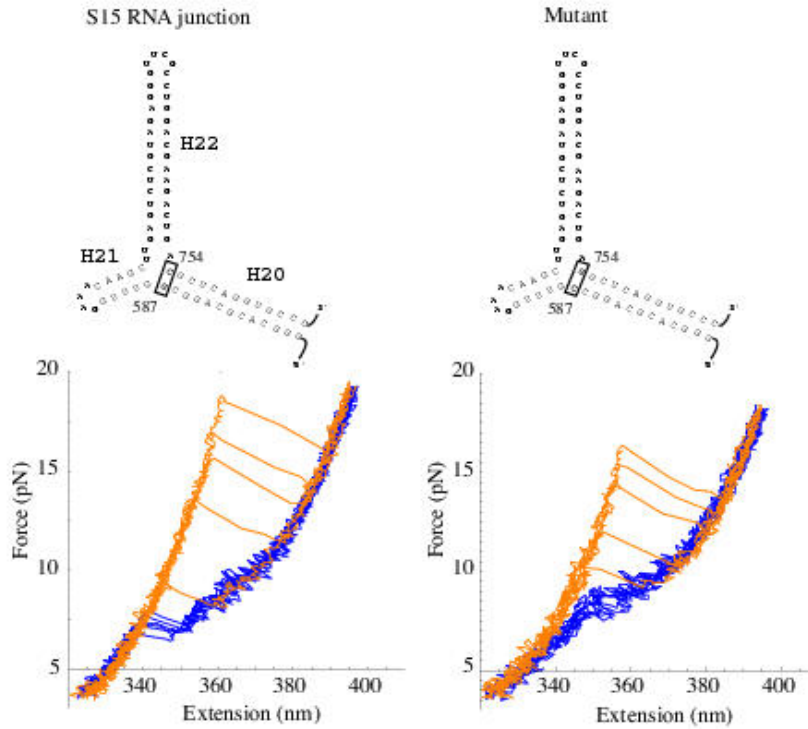


FIGURE S4

Figure S4. Secondary structures of the three-helix junction in the wild type and the C754G-G587C mutant. Five typical force-extension curves of unfolding (orange) and refolding (blue) reactions (62 mM KCl, 10 mM HEPES pH 7.8) are shown for both cases.

As shown in Table 1, cumulant methods do not even predict correctly the sign of the free-energy difference ($\Delta\Delta G_0^{(\text{exp})} = -2.8k_B T$) whereas the Jarzynski equality gives less

accurate free-energy values, with larger statistical uncertainties. Only by averaging the free-energy estimates obtained for the unfolding and refolding paths (called $W_J^{(est)}$ in Table 1, main text) can we get comparable values.

Unlike the hairpin, sometimes the three-helix junction (wild and mutant) does not refold into its native state, but into an intermediate conformation. The presence of the intermediate is revealed by the subsequent unfolding of the molecule which shows a completely different force-extension curve that cannot be aligned to the worm-like chain reference curve. We have excluded these trajectories (typically around 5%) from our data as one of the conditions for the validity of Eq.(1) is the fact that the initial state during the unfolding process must be the equilibrium (or native) conformation. Because the wild type and the mutant molecules were attached to identical handles, the contributions of these handles and RNA stretching are the same for both. Therefore, these contributions subtract out when estimating the free-energy difference between the two molecules.

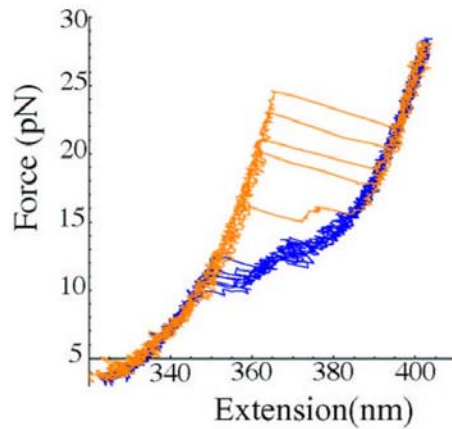


FIGURE S5

Figure S5. Typical force-extension curves for the wild type in the presence of Mg^{2+} ; five unfolding and refolding pathways are presented in orange and blue, respectively.

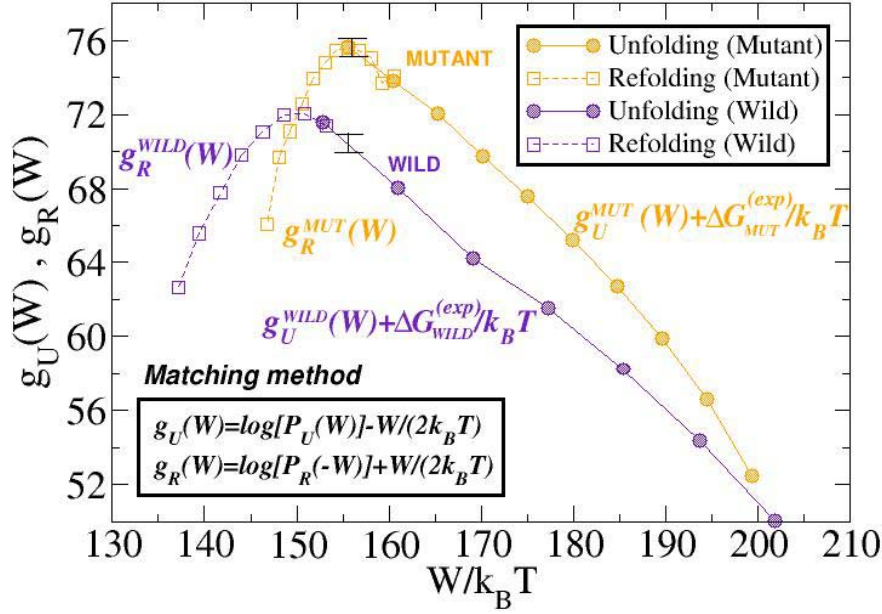


FIGURE S6

Figure S6. Matching method applied to the unfolding and refolding experimental work histograms as described in the text. The value of ΔG obtained is consistent with that extracted using the Bennett's acceptance ratio method¹³. We obtain $\Delta G = 154.1 \pm 0.4 k_B T$ and $\Delta G = 157.9 \pm 0.2 k_B T$ for the three-helix junction and the mutant, respectively. The thick black error bars show the vertical range along which matched distributions shift when changing the estimate for ΔG by $1 k_B T$.

Bennett's acceptance ratio method

When there is little overlap between the unfolding and refolding work distributions, an estimate of ΔG can be obtained with the *acceptance ratio method*, first proposed by Bennett in the context of equilibrium sampling¹³ and later extended by to the nonequilibrium case by Crooks¹⁸. To begin, note that Eq.(1) can be rewritten as,

$$f_x(W) \exp\left(-\frac{W}{k_B T}\right) P_U(W) = \exp\left(-\frac{\Delta G}{k_B T}\right) f_x(W) P_R(-W) \quad (4)$$

where $f_x(W)$ is an arbitrary real function, which depends on a parameter x . Integrating both sides of (4) between $W = -\infty$ and $W = \infty$ we get,

$$\left\langle f_x(W) \exp\left(-\frac{W}{k_B T}\right) \right\rangle_U = \exp\left(-\frac{\Delta G}{k_B T}\right) \langle f_x(W) \rangle_R \quad (5)$$

where $\langle \dots \rangle_U$ and $\langle \dots \rangle_R$ denote averages over work values sampled from the unfolding and refolding distributions, $P_U(W)$ and $P_R(-W)$, respectively.

This relation is valid for arbitrary functions $f_x(W)$. In particular, for $f_x(W) = 1$ we get the Jarzynski equality. If we further define,

$$z_U(x) = \log \left(\left\langle f_x(W) \exp\left(-\frac{W}{k_B T}\right) \right\rangle_U \right) \quad ; \quad z_R(x) = \log(\langle f_x(W) \rangle_R) \quad (6)$$

then we obtain the simple relation,

$$z_R(x) - z_U(x) = \frac{\Delta G}{k_B T} \quad . \quad (7)$$

Therefore the difference between both z functions must be a constant over all range of x values. Equation (7) is an exact relation if we were to know both unfolding and refolding work distributions with infinitely high precision. However, this is not the case in the experiments where there is noise in the measurements and only a finite number of measurements is available. Bennett has proven that, among all possible functions $f_x(W)$, the one that minimizes the statistical error of the estimate of ΔG is given by the function,

$$f_x(W) = \frac{\exp\left(\frac{x}{2k_B T}\right)}{1 + \exp\left(\frac{x - W}{k_B T}\right)} \quad . \quad (8)$$

Moreover, when the number of repeated experiments is the same along the unfolding and refolding paths, the best estimate is obtained by evaluating (7) at $x = \Delta G$ meaning that the best estimate for ΔG can be obtained from the intersection of the curves $y(x) = z_R(x) - z_U(x)$ and $y(x) = \frac{x}{k_B T}$. This result has been recently derived using maximum-likelihood methods by Pande and collaborators¹⁵. The results of the analysis for the hairpin and S15 (with and without magnesium) are shown in Figure S7.

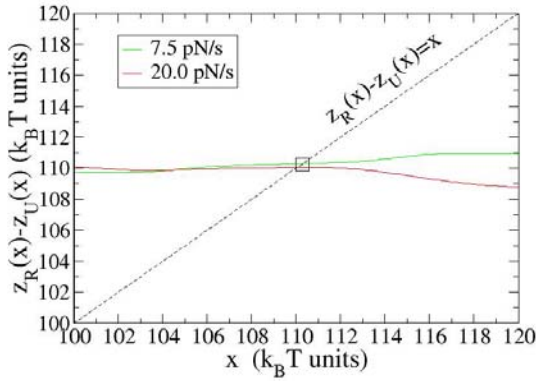


FIGURE S7(A)

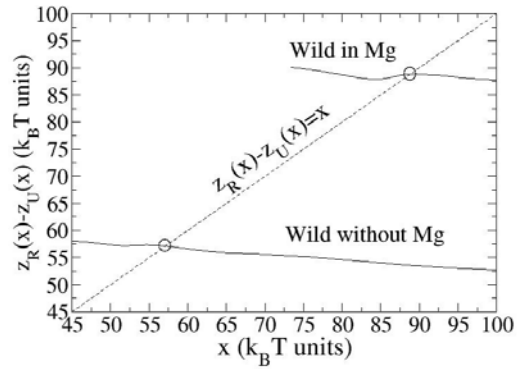


FIGURE S7(B)

Figure S7. Bennett's acceptance ratio method¹³ applied to different molecules. According to Eq. (7) the function $y(x) = z_R(x) - z_U(x)$ should intersect the dashed line $y(x) = x/k_B T$ at $x = \Delta G$. The former must be also approximately constant around the intersection region. (A) Hairpin at 7.5 and 20.0 pN/s (data shown in Figure 2, main text). Note that the function $y(x) = z_R(x) - z_U(x)$ is flat over a wide range of work (x) values. The small square indicates the crossing region located around $x = 110.3k_B T$. (B) S15 three-helix junction in the absence and with Mg^{2+} ions. The function $y(x) = z_R(x) - z_U(x)$ is very nearly flat around the crossing region (indicated by small circles) and shows the reliability of the method. The values obtained using this method are shown in Table 1.

Applicability of the method

Here we describe how general is the present method and under which conditions we expect it to be applicable to extract free energies. The main limitations to the method is for processes in which the system is removed too far from equilibrium with excessively large values of the dissipated work. We expect our method to be applicable as long as the amount of dissipated work (equal to the difference between the total irreversible work and the reversible or minimum work) is equal or less than $\sim 100 k_B T$. For large values of the dissipated work the experimental unfolding and refolding work distributions hardly cross, thereby limiting the direct applicability of the Crooks FT. Although the possibility to determine the crossing between the unfolding and refolding work distributions increases for a larger number of pulls, that number might soon become un-realizable in some cases. In general, a far better way to get reliable free energy estimates is by using quantitative data analysis such as the Bennett's acceptance ratio method used in this paper.

There are, however, at least two cases where, even for large values of the dissipated work, the method might still work. The first case corresponds to biomolecules that have transition states very close either to their folded or unfolded states. In this case we expect one among the two work distributions (unfolding or refolding) to be pretty wide and the other pretty narrow. The presence of a long tail in the one of the two work distributions might make it easier to infer the value of the reversible work at which the two distributions cross each other. This is the case of proteins with a high barrier located at less than 1nm distance from the folded state, and whose crossing constitutes the rate

limiting step for the unfolding dynamics. In addition, the protein can be characterized by a very corrugated free energy landscape with many competing basins of attraction or intermediates that slow down the folding dynamics. The unfolding work distribution would display, in this case, a very long left tail while the refolding distribution would be strongly peaked at smaller work values. The latter would dictate that the excursion of the molecule from the unfolded to the native state follows quite similar force-extension curves in every refolding realization, implying a reproducible collapse of the unfolded structure for every one of the repeated trajectories. Note that the scenario described above is what it is observed in our measurements on S15, suggesting more similarities than differences between the mechanical unfolding of proteins and RNAs¹⁹. The second case corresponds to biomolecular complexes that have a modular structure (e.g. RNAs made out of several domains). Application of our approach to recover the free energy landscape in such cases might be possible if the unfolding of different domains occurs in an approximate sequential fashion at different values of forces. In this way, the method could be applied by measuring the partial work at several intermediate forces corresponding to each of the unfolding intermediates. This approach would make it possible to reconstruct the free energy landscape for unfolding.

The applicability of the method to AFM pulling data could, however, be problematic. The stiffness of the AFM tip, which is typically 1000 times larger than that of the optical trap, may drive the system too far from equilibrium. In fact, the relevant parameter that tunes the degree of irreversibility induced by the pulling is the loading rate which is equal to the pulling speed times the stiffness of the AFM tip. Only by separating the tip from the

substrate at speeds around 1 – 10 nm/s we can expect the method to be applicable. AFMs have another limitation, however. For molecules with critical forces below 50 pN, the signal-to-noise ratio of the AFM might be too small to clearly define the transition events and accurately measure the work values along the pulls.

-
1. Liphardt, J., Onoa, B., Smith S. B., Tinoco, I. Jr. & Bustamante, C. Reversible unfolding of single RNA molecules by mechanical force. *Science* **292**, 733-737 (2001).
 2. Smith, S. B., Cui, Y. & Bustamante, C. An optical-trap force transducer that operates by direct measurement of light momentum. *Methods. Enzymol.* **361**, 134 (2003).
 3. Jarzynski, C. Nonequilibrium equality for free energy differences. *Phys. Rev. Lett.* **78**, 2690-2693 (1997).
 4. Liphardt, J., Dumont, S., Smith S. B., Tinoco, I. Jr. & Bustamante, C. Equilibrium information from nonequilibrium measurements in an experimental test of the Jarzynski equality. *Science* **296**, 1832-1835 (2002).
 5. Ritort, F., Bustamante, C. & Tinoco, I. Jr. A two-state kinetic model for the unfolding of single molecules by mechanical force. *Proc. Nat. Acad. Sci. USA* **99**, 13544-13548 (2002).
 6. Zuckerman, D. M. & Woolf, T. B. Theory of systematic computational error in free energy differences. *Phys. Rev. Lett.* **89**, 180602 (2002).
 7. Park, S. & Schulten, K. Calculating potentials of mean force from steered molecular dynamics simulations. *J. Chem. Phys.* **120**, 5946-5961 (2004).

-
8. Gore, J., Ritort, F. & Bustamante, C. Bias and error in estimates of equilibrium free-energy differences from nonequilibrium measurements. *Proc. Nat. Acad. Sci. USA* **100**, 12564-12569 (2003).
 9. Crooks, G. E. Entropy production fluctuation theorem and the nonequilibrium work relation for free-energy differences. *Phys. Rev. E* **60**, 2721-2726 (1999).
 10. Schurr, J. M. & Fujimoto, B. S. Equalities for the nonequilibrium work transferred from an external potential to a molecular system. Analysis of single molecule extension experiments. *J. Phys. Chem B* **107**, 14007-14019 (2003).
 11. Manosas, M. & Ritort, F. Thermodynamic and kinetic aspects of RNA pulling experiments, *Biophys. J.* in press.
 12. Hummer, G. & Szabo, A. Free-energy reconstruction from nonequilibrium single molecule experiments. *Proc. Natl. Acad. Sci. USA* **98**, 3658-3661 (2001).
 13. Bennett, C. H. Efficient estimates of free energy differences from Monte Carlo data. *J. Comp. Phys.* **22**, 245-268 (1976)
 14. Frenkel, D. & Smit, B. *Understanding molecular simulation*. (Academic Press, San Diego, ed. 2, 2002), Chapter 7.
 15. Shirts, R., Bair, E., Hooker, G. & Pande, V. S. Equilibrium free energies from nonequilibrium measurements using maximum likelihood methods. *Phys. Rev. Lett.* **91**, 140601 (2003).
 16. Hummer, G. Fast-growth thermodynamics integration: Error and efficiency analysis. *J. Chem. Phys.* **114**, 7330-7337 (2001).
 17. Ritort, F. Work and heat fluctuations in two-state systems: a trajectory thermodynamics formalism. *J. Stat. Mech: Theor. Exp.* P10016 (2004).

-
18. Crooks, G. E. Path-ensemble averages in systems driven far from equilibrium. *Phys. Rev. E.* **61**, 2361-2366 (2000).
 19. Thirumalai, D. & Hyeon, C. RNA and protein folding: Common themes and variations. *Biochemistry* **44**, 4957-4970 (2005).